ac currents in a vortex state of layered superconductors

S. E. Shafranjuk
Research Institute of Electrical Communications, Tohoku University, 2-1-1, Katahira, Aoba-ko, Sendai 980-77 Japan and Institute of Magnetism NANU, 36(b) Vernadskii av., Kiev, Ukraine

M. Tachiki
National Research Institute for Metals, 1-2-1 Sengen, Tsukuba 305, Japan

T. Yamashita
Research Institute of Electrical Communications, Tohoku University, 2-1-1, Katahira, Aoba-ku, Sendai 980-77, Japan

(Received 9 July 1997)

The ac properties of layered superconductors in the vortex state for the parallel orientation of the external magnetic field B are examined. We find that due to an intrinsic Josephson effect the ac characteristics depend on the kind of the steady-state fluxon structure. Both the collective mode Ω_{ps} and the ac penetration depth $\lambda_{\parallel}^{ac}(\omega,\mathbf{B})$ are affected by the magnetic field in an anomalous way, because of the reactive properties of the vortex state's environment. [S0163-1829(98)04801-2]

I. INTRODUCTION

In recent years the electromagnetic properties of metal oxide superconductors ($\widetilde{S}$) have received considerable attention. An increased interest to this issue has been prompted by observation of the low-lying collective mode in c polarized experiments[1–3] made on single crystal samples. A phenomenological theory of this phenomenum was proposed in Refs. 4,5. It was emphasized[4,5] that the layered structure of metal oxides caused a huge anisotropy of normal transport which is metalliclike within the ab planes while it is essentially nonmetallic and reduced in the c direction. According to Refs. 4,5, this nonmetallic character of the c axis transport as well as the Josephson nature of the coupling between the adjacent Cu-O planes is responsible for the low-lying collective oscillations with the frequency $\Omega_{ps} \leqslant \Delta, T_c$ (Δ is the energy gap value and T_c is the critical temperature). Since the intrinsic Josephson effect plays a key role in the formation of the collective mode, the mode itself should be affected by a dc magnetic field.[4–6] Actually, the model[4,5] predicts suppression of Ω_{ps} by the dc magnetic field, which depends on the magnitude and orientation of the magnetic induction vector $\mathbf{B}$ with respect to the crystal axis, i.e., on the type of vortex structure.[7–10] Nevertheless, when calculating the ac properties, the simplified phenomenological approach[4,5] operates with a few assumptions which are not evident for the mentioned case. Namely, the model[4,5] took into account the quasiparticle and Josephson components of the total interlayer ac current only, while basically, at finite temperatures and in a finite magnetic field, the so-called interference components[11] can be important as well. Besides, in the model,[4,5] the frequency dependence of the ac Josephson component was neglected while the quasiparticle component was assumed to obey the Ohm law. These assumptions, however, are not well consistent with a general picture of ac transport in weakly coupled systems because $\sigma(\omega)$ must be dependent on details of the low-energy electron spectrum [which apparently is the case in the metal oxide superconductors], and on the nature of c-axis transport as well. The contribution of the interference components into total ac current and the frequency dependence of all components were explored for $\widetilde{S}$ in the recent paper[12] within an interlayer tunneling model. It was shown[12] that the transverse collective mode observed in experiments[1–3] is determined by the balance between different components of the electric current (the quasiparticle, Josephson, and two interference components). The calculations performed in Ref. 12 were related, however, to a specific tunneling model in absence of any dc external fields. Since applied dc magnetic field may create a mixed state having a complex structure also affecting the Josephson component of the total c-axis transport, the ac properties of layered superconductors (SC's) at $\mathbf{B} \neq 0$ is a matter of interest.

In this paper, solving the system of nonlinear equations for the interlayer phase difference, we analyze the effect of dc magnetic field $\mathbf{B} \neq 0$ on ac properties of a layered superconductor in the vortex state, for a parallel orientation of the dc magnetic field [so-called fluxon lattice]. We would like to account for the contribution from all the aforementioned components of electric ac current at finite temperatures. We will show that as $\mathbf{B}$ increases, the frequency of the transverse collective mode Ω_{ps} is depressed. In Sec. II, we formulate the main assumptions of the model and basic equations, while in Sec. III we compute the distribution of supercurrent and of local dc field in the fluxon structure. We also calculate the distribution of the in-plane supercurrent j_x^n over the stack. In Sec. IV, we present results of numerical calculations of $\Omega_{ps}(\mathbf{B})$ and examine the ac penetration depth along the c axis $\lambda_{\parallel}^{ac}(\omega,\mathbf{B})$ (at fixed frequencies), which shows quite remarkable features due to reactive properties of mixed state. For comparison, we compute the same characteristics for an unconventional layered superconductor.

II. BASIC EQUATIONS

The ac properties of layered superconductors in mixed state are explored here considering the system as a stack of

Josephson junctions. In metal oxide single crystals, such microscopic junctions are naturally formed by Cu-O superconducting layers separated by interstitial insulating (or normal) regions. Then the c-axis electric current can be described in terms of interlayer electron tunneling, which in stationary case consists of the dc Josephson component only. The superfluid current density can become quite inhomogeneous if a constant magnetic field applied to the type-II superconductor creates a certain vortex structure inside it. The gestalt of the mixed state taking place in these superconductors depends on the magnitude of the external parallel magnetic field $\mathbf{B}$ as well as on the strength of the Josephson interlayer coupling, and on the temperature T. Initial theoretical models for the vortex state in weakly coupled layered SC's were proposed in Refs. 7–10. It was shown that both, very high anisotropy and the Josephson interlayer coupling in the metal oxides are significant for the formation of fluxon lattice.[8,9] As was emphasized in the Refs. 8–10, the alternation of the order parameter amplitude $|\Delta(\mathbf{r})|$ does not contribute essentially to the total free energy, because when $\mathbf{B}\perp c$ axis, the vortex cores [for which, however, $|\Delta(x)|\neq 0$] are localized in the interlayer interstitial regions. Another reason is that the magnitudes of coherence length $\xi_\perp$ and ξ_{ab} (in the c direction and within the ab plane, respectively), are always much smaller than the magnetic field penetration length. The mentioned circumstances allow to neglect the contribution due to $|\Delta(\mathbf{r})|$ variations when calculating averaged characteristics. The equations for the order parameter follow from the free energy functional[8–10] describing the SC with Josephson interlayer coupling in the magnetic field, or from Maxwell equations taking into account the Josephson relationship. In this paper, the main attention is paid to the case of parallel field [$\mathbf{B}\| ab$ planes], and the stationary ''vortex'' part of interlayer phase differences $\varphi_{n,n+1}$ is described by the set of extended sine-Gordon equations[8–10]

$$\nabla_x^2\varphi_{n,n+1}-\frac{1}{\lambda_J^2}[2\sin\varphi_{n,n+1}-\sin\varphi_{n+1,n+2}-\sin\varphi_{n-1,n}]-\frac{1}{\lambda_\perp^2}\sin\varphi_{n,n+1}=0, \tag{1}$$

where $n=\overline{0\cdots N}$ denotes the index of layer, N is the number of layers in the crystal; $\lambda_J=\gamma c_\perp$, $\gamma=\lambda_\perp/\lambda_\|$ is the anisotropy ratio, and $\lambda_\perp$ and $\lambda_\|$ are the static penetration depths along the c axis and ab plane, respectively. Thus, in the presence of pinned vortices induced by the parallel dc magnetic field, the phase difference due to external weak ac field $\phi^{\rm ac}_{n,n+1}(t)$ can be considered as a small addition to the main ''steady state vortex'' part, $\varphi_{n,n+1}$

$$\phi_{n,n+1}(t)=\varphi_{n,n+1}+\phi^{\rm ac}_{n,n+1}(t). \tag{2}$$

The ac part $\phi^{\rm ac}_{n,n+1}(t)$ itself is determined from the Josephson relationship

$$\phi^{\rm ac}_{n,n+1}(t)=2ed_b\int^t dtE_z(t), \tag{3}$$

where $d_b\simeq c_\perp$ is the averaged thickness of the interstitial regions, and $E_z(t)$ is the c axis component of the electric field vector. When computing ac characteristics, one may take into account that spatial variations of $|\Delta(\mathbf{r})|$ occur on a short scale $\sim\xi_\perp$ (or ξ_{ab}) while the $\varphi_{n,n+1}(x)$ alternates on much longer scale $\sim\lambda_J$ (or even $\lambda_\perp$). If the concentration of impurities and crystal lattice deffects is small, and $B\ll B_{c2}$ (the concentartion of vortices is also small), then the total area of regions with the reduced magnitude of $|\Delta(\mathbf{r})|$ is negligible. Practically it means that one can simply set $|\Delta(\mathbf{r})|\equiv\Delta=$const. Additionally, for the far-infrared frequencies $\omega\sim\Delta,T_c$ one may still have $\lambda_{\rm field}\gg c_\perp$ ($\lambda_{\rm field}$ is the wave length of the ac field; and $c_\perp$ is the c-axis lattice constant). The last condition, indeed, is even better satisfied for the microwave measurements,[6] where $\omega<<\Delta,T_c$. Thus, one can implement an approximation considering the ac field to be homogeneous on the scale $\sim c_\perp$. The dc magnetic field, however, creates a vortex structure providing inhomogeneity on the scale of intervortex distance. In many experiments the main interest is paid to the characteristics averaged over the volume of sample (e.g., in c polarized far-infrared measurements,[1–3] and moreover, in microwave experiments[6]), with the size $d_{\rm sample}\gg\lambda^{\rm ac}_\perp(0)$ and $\lambda^{\rm ac}_\|(0)$ [$\lambda^{\rm ac}_\perp(0)$ and $\lambda^{\rm ac}_\|(0)$ being the ac penetration depths at $T=0$]. The discussed distinction in scales suggests that one can simplify the description separating the dc and ac contributions to the electric current from each other. Then the total c-axis current is

$$j_{z,n}(t)=j^{(0)}_{z,n}+j^{(1)}_{z,n}(t) \tag{4}$$

$$j^{(1)}_{z,n}(t)=\int dt'\sigma_\perp(t,t')E_z(t')=-\frac{\hbar}{2ec_\perp}\int dt'\frac{\partial\sigma_\perp(t,t')}{\partial t'}\phi^{\rm ac}(t')=-i\frac{\hbar}{2ec_\perp}\omega\sigma_\perp(\omega)\phi^{\rm ac}_\omega e^{i\omega t}, \tag{5}$$

where the c-axis dc current is assumed to be purely of Josephson nature, $j^{(0)}_{z,n}=j_c\sin[\varphi_{n,n-1}(x)]$, while the second ac term $j^{(1)}_{z,n}(t)$ contains four contributions coming from quasiparticle and Josephson (active and reactive) components of electric current. In this approximation, the variations of dc current in fact are fully determined by the interlayer phase difference $\varphi_{n,n+1}(x)$ [which for a pinned fluxon structure can be found solving the stationary Eq. (1)], while the small ac current can be calculated separately from a microscopic model. For the average over the sample active $\sigma_{\perp 1}$ and reactive $\sigma_{\perp 2}$ components of the c-axis ac conductivity, one writes the following general expressions:

$$\sigma_{\perp 1}(\omega)=\sigma_{\rm qp}(\omega)+\sigma_{\rm Jos,2}(\omega)\langle\cos\varphi_{n,n+1}\rangle_s-\sigma_{\rm Jos,1}(\omega)\times\langle\sin\varphi_{n,n+1}\rangle_s, \tag{6}$$

$$\sigma_{\perp 2}(\omega)=\sigma_{\rm Jos,1}(\omega)\langle\cos\varphi_{n,n+1}\rangle_s+\sigma_{\rm qp,1}(\omega)+\sigma_{\rm Jos,2}(\omega)\times\langle\sin\varphi_{n,n+1}\rangle_s, \tag{7}$$

where $\sigma_{\rm qp}(\omega)$ is the part of ac conductivity related to the contribution from quasiparticle tunneling $\sigma_{\rm Jos,1}(\omega)$ is the ac Josephson component $\sigma_{\rm Jos,2}(\omega)$ is the so-called interference component (which is due to the interference between the

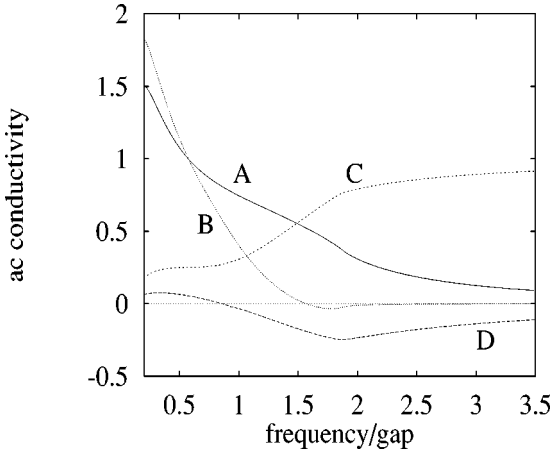

FIG. 1. The components of ac conductivity at $T/\Delta_0 = 0.4$.

superfluid and quasiparticle tunneling, and provides the contribution to the electric current $\sim \cos \varphi_{n,n+1}$, see, e.g., Ref. 11), $\sigma_{\mathrm{qp},1}(\omega)$ is the so-called quasiparticle ''extractive'' component (this component is related to the tunneling ''extraction'' of quasiparticles), and $\langle \ldots \rangle_s$ means the averaging over the volume of sample. One can perform the calculation of components of the ac conductivity in the linear response approximation within the tunneling model, similarly as it was done, e.g., in Refs. 11,12. For certainity we use an ordinary assumption that the normal state ab-plane electron transport is metalliclike while the c-axis transport has an ''incoherent'' tunneling nature (i.e., the tunneling matrix element[11] $T_{pp'}$ does not depend on electron momentum $\mathbf{p}$ $T_{pp'} = T \equiv \mathrm{const}$), and that superconductivity in the ab planes can be described within the BCS approximation. Then the normalized tunneling conductivity $\sigma_\perp(\omega,T)/\sigma_{\perp N}$ ($\sigma_{\perp N}$ is the c-axis normal-state conductivity), in fact is a universal function which depends only on the symmetry of supeconducting order parameter $\Delta(\mathbf{p})$ as well as on the normalized parameters $\overline{\omega} = \omega/\Delta_0$ and $t = T/T_c$, $T_c = 2\Delta_0/3.5$, and Δ_0 is the maximum magnitude of $\Delta(\mathbf{p})$ at $T = 0$. For illustration, we plot the functions $\sigma_{\mathrm{Jos},1}(\omega)$ (curve A), $\sigma_{\mathrm{qp},1}(\omega)$ (curve B), $\sigma_{\mathrm{qp}}(\omega)$ (curve C), and $\sigma_{\mathrm{Jos},2}(\omega)$ (curve D) in Fig. 1 for the $d_{x^2-y^2}$ symmetry of $\Delta(\mathbf{p})$. From formulas (6) and (7) one can infer that due to the factors $\langle \cos \varphi_{n,n+1} \rangle_s$ and $\langle \sin \varphi_{n,n+1} \rangle_s$, the ac conductivity in the vortex state may have more complex structure compared to the zero field case, $\mathbf{B} = 0$. These factors determine the balance between the Josephson and interference parts, contributing to the total ac current in the system. In case of s wave pairing, according to Ref. 11, at $T \to 0$, and $\omega \to 0$, there is a contribution from $\sigma_{\mathrm{Jos},1}$only. Then the total current consists of the Josephson component[5] alone. However, at finite T and ω (and moreover for the d-wave pairing symmetry), this kind of assumption[5] is not valid anymore, and one has to account for contributions from the quasiparticle and interference processes[12] as well. It is essentially important in a finite magnetic field $\mathbf{B} \neq 0$ which suppresses the ac Josephson ($\propto \sigma_{\mathrm{Jos},1}$) and interference ($\propto \sigma_{\mathrm{Jos},2}$) parts of total current as dc field grows up to H_0. Henceforth we shall see that at $B \sim H_0$ ($H_0 = \Phi_0/\lambda_\perp c_\perp$; Φ_0 is the flux quantum) the contribution of the quasiparticle and interference components even increases.

III. DISTRIBUTION OF dc SUPERCURRENT IN THE FLUXON LATTICE

When a steady state vortex structure is created by the external magnetic field $\mathbf{B} = (0, B_y, 0)$, the supercurrent density becomes quite inhomogeneous inside the sample causing an alternation of average Josephson energy versus the field strength. In a stack of Josephson junctions, in the presence of fluxon lattice, basically one can not assume that the averaged dc supercurrent [the Josephson part of which is $\propto \langle \sin \varphi_{n,n+1} \rangle_s$] is equal to zero. It means therefore that there is a dependence of ac characteristics on the configuration of vortex lattice. Here we shall not conduct any general classification of fluxon structures, leaving the detailed delineation for elsewhere. Instead we concentrate our attention on calculating $\langle \sin \varphi_{n,n+1} \rangle_s$ from a particular solution of Eq. (1), using appropriate boundary conditions at the edges of the unit cell. The influence of the constant magnetic field on the ac properties is apparent already from Eq. (6), which contains the factors $\langle \sin \varphi_{n,n+1} \rangle_s$, and $\langle \cos \varphi_{n,n+1} \rangle_s$ (the last one is related to the Josephson energy). In order to determine those averages, $\langle \sin \varphi_{n,n+1} \rangle_s$, and $\langle \cos \varphi_{n,n+1} \rangle_s$, one has to implement a particular solution, $\varphi_{n,n+1}(x)$, of Eq. (1). Equation (1) must also be completed by the condition which fixes the positions of the vortices. Usually it is assumed that in a parallel dc magnetic field, the centers of vortices form a triangular lattice,[10] the parameters of which are determined by the condition that the magnetic flux is Φ_0 per vortex. This kind of assumption is apparent, e.g., for the lattice formed by Abrikosov vortices. However, in the marginally anisotropic and nonlinear layered system, such as a metal oxide single crystal, the above guess must better be verified by extensive direct calculations. Unfortunately, any analytical solution of Eq. (1) can be obtained only in limiting cases (see, i.e., Ref. 10), which have very modest practical utility. Therefore we find a steady state solution numerically. A numerical approach was used before by authors of Ref. 15, but they considered mostly nonstationary states while the results were reported for a stack of only $N = 5$ junctions, which is not sufficient in our case. Here we solve Eq. (1) for a stack of $N = 50$ Josephson junctions (we also performed calculations for a stack of $N = 100$ junctions, and they show the same tendencies). Then we would like to use the found solution for the calculation of aforementioned factors $\langle \sin \varphi_{n,n+1} \rangle_s$ and $\langle \cos \varphi_{n,n+1} \rangle_s$. In this paper we implemented the following boundary conditions. Since we are looking for the periodic solution along the $\hat{x}$ direction, we assumed that the local magnetic induction $B_y^{\mathrm{loc}}(x)$ is a periodic function of x with period $a_x = \Phi_0/B_y l c_\perp$. The integer number l entering the last formula was introduced to describe commensurable states of the vortex lattice (see, e.g., Refs. 8,9, where it was assumed that in a general case the lattice may contain the vortices not in every adjacent layer but, e.g., in every lth layer, and then $a_x = \Phi_0/B_y l c_\perp$) . Here we use the parameter l to quote the junctions in the stack, in which we put fluxons via boundary conditions. It is achieved by setting $\varphi_{n,n+1}(x)|_{x=x_l} = \pi$ for the quoted junctions. For instance, $l = 2$ means that we put a fluxon into each third junction (the boundary condition in this case is of kind $\cdots 00\pi 00\pi 00\pi 00 \cdots$). Additionally, at the edge of the unit cell along the a axis we have $\nabla_x \varphi_{n,n+1}(x)|_{x=x_l,x_r} =$

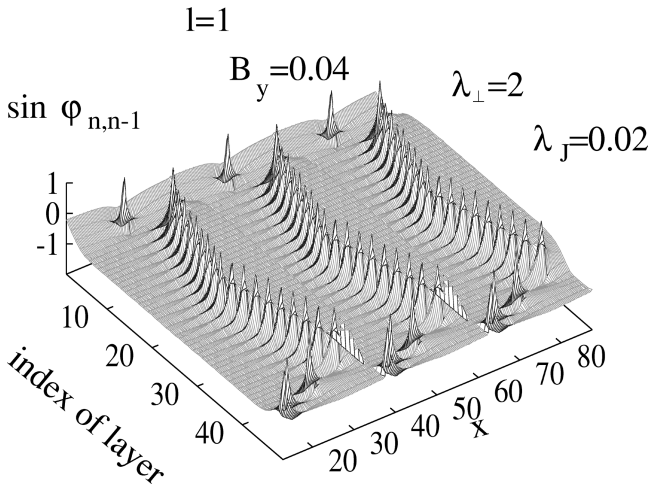

FIG. 2. The distribution of the dc supercurrent density $\sin\varphi_{n,n+1}(x)$ at $B_y=0.04$ for the three a-axis unit cells in a stack of Josephson junctions induced by the applied parallel field.

$(2ec_\perp/\hbar)B_{uc}$, where $x_l(x_r)$ is the left (right) edge of the unit cell, $x_r=x_l+a_x$, and the parameter B_{uc} is related to the external dc magnetic field. For the calculations we set $B_{uc}=B_y$. Then we proceed the integration of Eq. (1) along $\hat{x}$ between x_l and x_r, considering it as a system of first order differential equations. As a first step, we integrate Eq. (1) with ascending x, and calculate $\varphi_{n,n+1}(x=x_r)$. Then using, $\varphi_{n,n+1}(x=x_r)$ as a new boundary condition, together with $\nabla_x\varphi_{n,n+1}(x)|_{x=x_l,x_r}=(2ec_\perp/\hbar)B_{uc}$ we move in the opposite direction with descending x, from x_r to x_l. In this way, we repeat the procedure until a stable solution is achieved. In Fig. 2 we show a three-dimensional plot for the interlayer Josephson current $j_z^{n,n-1}\propto\sin\varphi_{n,n+1}$ versus the x coordinate and the index of junction, computed from the solution of Eq. (1) for the mentioned stack. Contrary to our expectations, and to results of Refs. 10,15, one can see that instead of triangular lattice the fluxons form an array of chains, ordered along the c axis and periodic along the a axis. From Fig. 2, one also can infer that the fluxons are quite spatially localized and are distinguished by sharp tails with a core width $d_{fl}\sim 0.7$ ranging between λ_J and $\lambda_\perp$ (for the plot we used the following parameters: $l=1$, $\lambda_J=0.02$, $\lambda_\perp=2$, and $B_y=0.04$, we considered three unit cells to display the periodicity of the supercurrent density distribution). The applied magnetic field B_y is expressed in units of $\Phi_0/(\eta c_\perp^2)$, $\eta=5\times10^3$ at ($c_\perp=1$ nm it corresponds to $\Phi_0/\eta c_\perp^2=0.4$ T) then the period of the fluxon structure along the a axis is $a_x=1/(lB_y)$. The profile and the structure of a separate fluxon is somewhat similar to that obtained, e.g., in Refs. 16,17 for a single Josephson junction. The values for penetration depths are expressed here in dimensionless units, in which the c-axis lattice constant corresponds to $c_\perp\simeq2\times10^{-4}$. Those units are chosen only for the better illustration (e.g., the fluxon core size in those units is ≈ 1). Alternating the magnetic induction B_y and the parameter l one obtains various configurations which correspond to local minimums of the free energy in the Lawrence and Doniach model, and which, however, have a common feature: they are periodic and consist of buckled chains of fluxons. The buckling is determined by the size a_x of the unit cell (i.e., by the magnetic induction). Thus

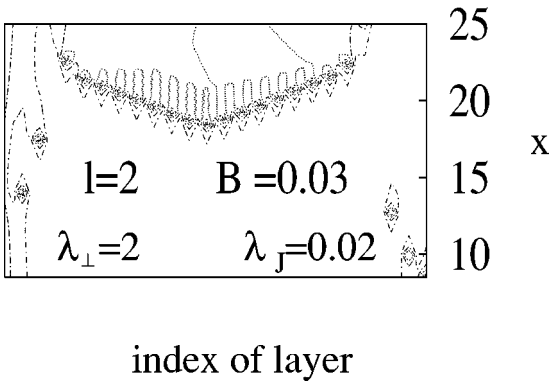

FIG. 3. The distribution of local magnetic field $B_{y,n}^{\rm loc}(x)$ for one unit cell. The dashed lines show the contours for equivalent values of $B_{y,n}^{\rm loc}(x)$.

the variation of the boundary condition shifts only the phase of a buckled chain and does not make sense in the infinite limit. Similar buckled chains of vortices were observed by means of the Bitter-pattern technique in Ref. 18 for a $Y_1Ba_2Cu_3O_7$ single-crystal sample in a parallel magnetic field. Though the initial interpretation[19] of the experiment[18] was given in terms of Abrikosov vortices considered within the phenomenological London model, in our opinion, this kind of approach[19] is highly controversial for the layered superconductor with an intrinsic Josephson effect. Instead, the application of the Lawrence and Doniach model is more logistic in this case.

Combining the Maxwell equations and the obtained solution, one can compute the distribution of the local dc magnetic induction in our setup as

$$B_{y,n}^{\rm loc}(x)=j_0\frac{4\pi}{c}\int_{-\infty}^{x}\sin[\varphi_{n,n+1}(x)]dx, \tag{8}$$

where j_0 is the maximal current density, while the a-axis component of the dc supercurrent density is obtained from the continuity equation $(\nabla,[\hat{z}\cdot j_z^{n,n-1}+\hat{x}\cdot j_x^n])=0$, as

$$j_x^n(x)=-\int_0^x\delta^{(1)}j_z^{n,n-1}(x)dx, \tag{9}$$

where $\delta^{(1)}$ is the first-order finite difference operator, i.e., $\delta^{(1)}f_n=(f_n-f_{n-1})/c_\perp$; f_n being an arbitrary function. In order to compare our results with the Bitter-pattern experiment,[18] in Fig. 3 we show the contour plot for the distribution of the local dc magnetic induction $B_{y,n}^{\rm loc}(x)$ obtained for $B_y=0.03$ and $l=2$. The dashed lines in this plot show contours for equivalent values of $B_{y,n}^{\rm loc}(x)$. From the plot one can also see, that the field penetrates through the fluxons in the way, which is dissimilar to that taking place for the Abrikosov vortices, where the field penetrates via the vortex core. Figure 4 presents the three-dimensional (3D) plot for the distribution of the a-axis dc supercurrent density $j_x^n(x)$ for the same parameters as in Fig. 2. In this plot we present only one period in $\hat{x}$ direction. From the mentioned figure one can see, that the chain of fluxons is reflected also in the $j_x^n(x)$ distribution, however the maximums of $j_z^{n,n-1}(x)$ are replaced by minimums (which indeed are negative) of $j_x^n(x)$ instead.

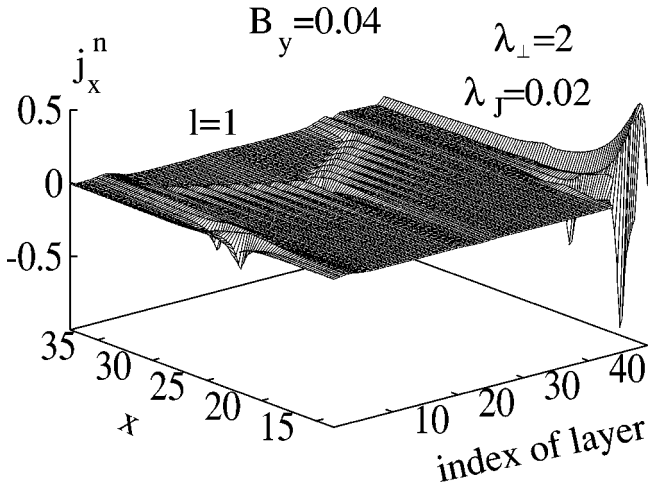

FIG. 4. The distribution of the ab-plane component of the supercurrent.

Departing from the above discussed solution, we calculate average values of the factors $\langle \sin \varphi_{n,n+1} \rangle_s$ and $\langle \cos \varphi_{n,n+1} \rangle_s$, which are necessary to obtain ac characteristics. Initially we examine an illustrative limiting case of a small sample with dimensions $L_x, L_y \ll \lambda_\perp, \lambda_J$. In this limit, the interlayer phase difference is

$$\varphi_{n,n+1}(x) \simeq 2\pi \frac{\Phi}{\Phi_0} \frac{x}{L_x} + \varphi_0 \tag{10}$$

(Φ is the magnetic flux) and one obtains a familiar Fraunhofer pattern[9] for the field factors $\langle \sin \varphi_{n,n+1} \rangle_s$, $\langle \cos \varphi_{n,n+1} \rangle_s$ entering into Eqs. (6) and (7) (in fact the factors are related to a maximal current of each interlayer junction):

$$\langle \sin \varphi_{n,n+1} \rangle_s = \langle \cos \varphi_{n,n+1} \rangle_s = \frac{\sin z}{z}, \tag{11}$$

where

$$z = \pi \frac{B_y}{B_0}, \quad B_0 = \frac{\Phi_0}{L_x c_\perp}. \tag{12}$$

One could expect that the spatial average of the functions $\cos[\varphi_{n,n+1}(x)]$ and $\sin[\varphi_{n,n+1}(x)]$ over the sample calculated from the above obtained solution (see Fig. 2) must give, at certain conditions, a similar pattern. Of course, for a big sample with a size $L_x, L_y \gg \lambda_\perp, \lambda_J$, the Fraunhofer pattern, generally speaking, is hardly observable, because as B_0 becomes small, the oscillations cannot be well distinguished. Additionally, the pattern could be spoiled due to fluxons entering the junction in an irregular way.[9] However, in our case the vortex structure is formed by chains of fluxons deployed into the sample in a collective way. In this case, because of the regularity of the steady state solution $\varphi_{n,n+1}(x)$, the contribution to the factors becomes oscillating as well. This kind of oscillation is visible Fig. 5, where we compare the factors $\langle \cos \varphi_{n,n+1} \rangle_s$ versus B_y calculated for a small sample from formula (11) (curve 1) and for fluxon structures calculated for $l=1$, $\lambda_J=0.02$, $\lambda_\perp=2$ (curve 2). In the calculations, the sample size along the a axis was taken as $L_x=8\lambda_\perp$. We notice, that as field alternates, the regular steady state fluxon structure is modified and rearranged becoming different from

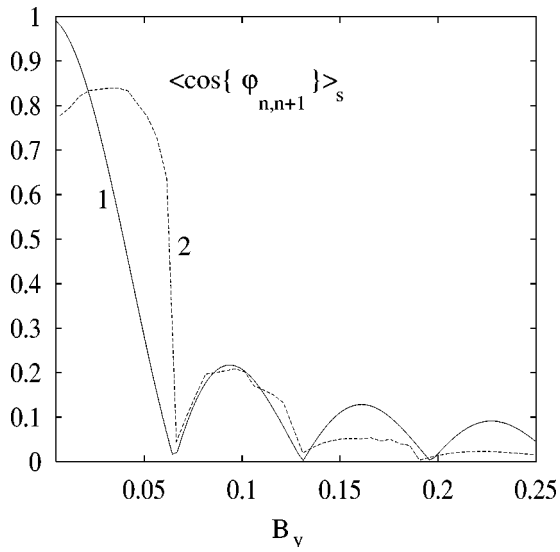

FIG. 5. The dc magnetic field dependence of the factor $\langle \cos \varphi_{n,n+1}(x) \rangle_s$ for the small (curve 1) and big (curve 2) samples.

that shown in Fig. 2, which corresponds to a particular case at $B_y=0.04$. This evolution of the fluxon structure produces kinks in curve 2, which it is not as smooth as curve 1 for an idealized case. In the next section we use these factors to compute the magnetic field dependence of the resonance frequency $\Omega_{ps}(\mathbf{B})$ and the ac penetration depth, $\lambda_\parallel^{ac}(\omega, \mathbf{B})$.

IV. THE c-AXIS COLLECTIVE OSCILLATIONS IN dc MAGNETIC FIELD

The above Eqs. (6) and (7) for $\sigma_{1,2}(\omega)$ with the calculated field factors allow us to explore ac characteristics of a layered superconductor in a dc magnetic field. The most interesting issues which are currently under discussion[1–7,12,13] are related to the collective oscillations and to the ac penetration depth. Here we assume that the dc magnetic field is directed along the $\hat{y}$ axis while the vector of transverse ac electric field is along the $\hat{x}$ axis. At finite temperatures and in the case of anisotropic pairing which we would like to delineate here, the collective mode is determined[12] by a balance of different components of the electric current in conditions of low c-axis conductivity and a relatively high dielectric con-

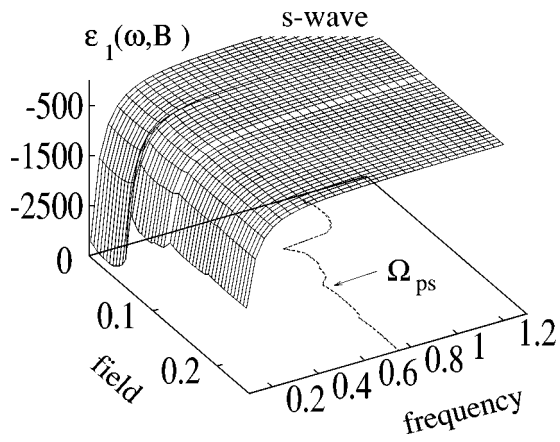

FIG. 6. 3D plot of $\mathrm{Re}\{\epsilon^\perp(\omega, \mathbf{B})\}$ for the s stack. The dc magnetic field dependence of $\Omega_{ps}(B)$ is evident from the contour.

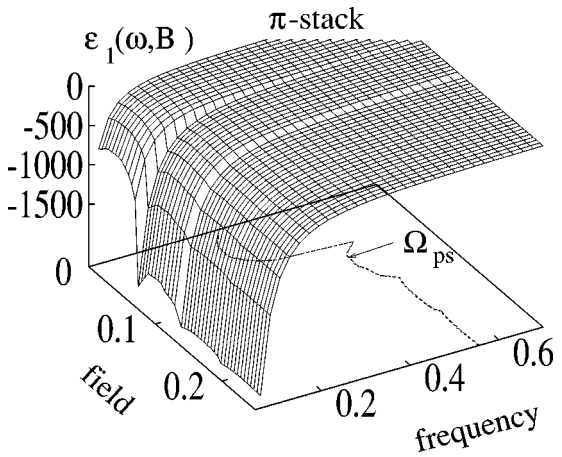

FIG. 7. The same 3D plot as before but for the π stack.

stant. The transverse dielectric function then is defined as

$$\epsilon^{\perp}(\omega)=\left[\epsilon_{\infty}-\frac{4\pi i\sigma_{\perp}(\omega,\mathbf{B})}{\omega}\right], \tag{13}$$

where $\sigma_{\perp}(\omega,\mathbf{B})$ is the linear response ac conductivity in the lateral c-direction which is to be found from microscopic calculations [namely from formulas (6) and (7)]; ϵ_{∞} is the high-frequency dielectric constant. In this paper we confine ourselves to study in details the effect of the dc magnetic field in the homogeneous interlayer ac current $\propto\sigma_{\perp}(\omega,\mathbf{B})$. The resonance frequency Ω_{ps} is determined from the general condition

$$\mathrm{Re}\{\epsilon^{\perp}(\omega=\Omega_{ps},\mathbf{B})\}=0 \tag{14}$$

at an assumption that $\mathrm{Im}\{\epsilon^{\perp}(\omega=\Omega_{ps},\mathbf{B})\}$ is small. From Eqs. (13) and (14) one can see that Ω_{ps} depends on the dc magnetic field via $\sigma_{\perp}$. Therefore, to determine $\Omega_{ps}(\mathbf{B})$, one has to compute $\sigma_{\perp}(\omega,\mathbf{B})$, using the factors $\langle\cos\varphi_{n,n+1}\rangle_s$ and $\langle\sin\varphi_{n,n+1}\rangle_s$, which were found from the solution $\varphi_{n,n+1}(x)$ of Eq. (1) in Sec. II. The numerical calculations of $\mathrm{Re}\{\epsilon^{\perp}(\omega,\mathbf{B})\}$ were performed in a similar way as it was described in Refs. 12,14, accounting for the cases of different symmetry of the order parameter $\Delta(\mathbf{p})$ ($\mathbf{p}$ is the electron momentum). We challenge the following stacks of Josephson junctions: (i) s stack (s-wave SC), (ii) g stack (anisotropic s-wave), and (iii) π stack [d wave with an antiphase orientation of $\Delta(\mathbf{p})$ petals in adjacent layers[12]]. Let us note that when calculating the ac characteristics for the π stack, one must use a different steady state solution than for cases (i) and (ii). The equation for $\varphi_{n,n+1}(x)$ in case (iii) is similar to Eq. (1), but has a reversed sign of the Josephson current contribution. To compute the function $\mathrm{Re}\{\epsilon^{\perp}(\omega,\mathbf{B})\}$ for the s wave symmetry of the order parameter [s stack] plotted in Fig. 6, we used the following parameters which are expressed in values of the order parameter magnitude $\Delta_0=\Delta(T=0)$. Particularly, in these units $\sigma_{N\perp}=0.7$ ($\sigma_{N\perp}$ is the average normal state interlayer tunneling conductivity) which corresponds to the value 1.6 Ω^{-1} cm^{-1} (this is a typical magnitude of $\sigma_{N\perp}$ for the single-crystal samples of $La_{2-x}Sr_xCuO_4$ used in far infrared c-polarized experiments[1,3]) and the temperature $T=0.12$, $\epsilon_{\infty}=23$. From Fig. 6 one can see that the frequency and dc magnetic field dependence of $\mathrm{Re}\{\epsilon^{\perp}(\omega,\mathbf{B})\}$ is quite spectacular. The crossing by this function of the plane $\mathrm{Re}\{\epsilon^{\perp}\}=0$ is shown in the figure by the contour. This contour defines the resonance frequency of the collective mode $\Omega_{ps}(B)$ which in accordance with Fig. 6 is sharply depressed at the field $B_y\simeq 0.07$. This sharp drop in the resonance frequency is related to the first maximum in the Fraunhofer pattern (see Fig. 5). Then $\Omega_{ps}(B)$ becomes slightly oscillating as the field grows. The behavior $\Omega_{ps}(B)$ is saturated at fields $B_y\approx 0.3$, and $\Omega_{ps}(B)$ remains finite in these fields though even $\langle\cos\varphi_{n,n+1}\rangle_s\approx 0$. The finite value of $\Omega_{ps}(B)$ is caused by so-called ''extractive'' tunneling contribution [namely, by $\sigma_{\mathrm{Jos},1}$ in formulas (6),(7)] which was usually neglected before (see Refs. 5). Calculations show that similar dependence $\Omega_{ps}(B)$ (although with a smaller magnitude of the resonance frequency) takes place also for a g stack. As is evident from Fig. 7, the picture is different for the π stack. There one can observe that $\Omega_{ps}(B)$ at small fields is decreased as well, but instead of saturation at $B_y\geqslant 0.03$ it turns to increase, having a maximum at $B_y\simeq 0.07$. Then $\Omega_{ps}(B)$ oscillates versus B_y, up to $B_y\simeq 0.3$ at which it becomes finally saturated. The evolution of the vortex structure under the external dc field influence

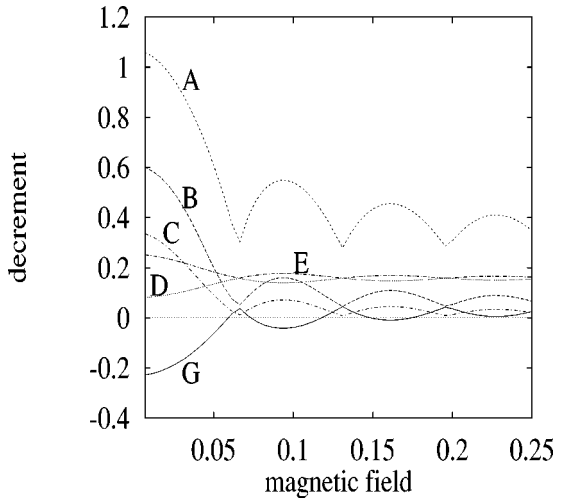

FIG. 8. The dc field dependence of the ac field decrement $\mathrm{Im}\{k_{ab}(B_y)\}$ for a small sample with a flux quantization effect.

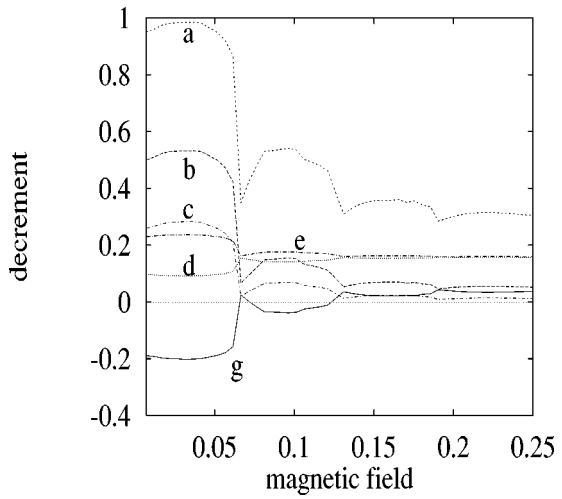

FIG. 9. The dc field dependence of the ac field decrement $\mathrm{Im}\{k_{ab}(B_y)\}$ for a big sample.

plays an important role for the penetration of ac fields into layered superconductors. This is illustrated by Figs. 8 and 9, where we present the dc field dependence of ac field decrement $\mathrm{Im}\{k_{ab}(B_y)\}$ [k_{ab} is a component of the wave vector $\mathbf{k}=(k_\perp, k_{ab})$; $k_{ab}(B_y)=(\omega/c)\sqrt{\epsilon^\perp(\omega,B_y)}$], which also is related to the ac penetration depth[20]

$$\lambda_\parallel^{\mathrm{ac}}(\omega,B_y)=\frac{1}{\mathrm{Im}\{k_{ab}(B_y)\}}. \tag{15}$$

The last formulas are related to a typical idealized setup considered in Refs. 12,13 which assumes a transverse polarization of the external field, and also that the wave vector **k** is parallel to layers while ac field vector **E** is along the c axis. Initially we examine an interesting limiting case of a small sample [see formulas (11), (12) for $\langle\sin\varphi_{n,n+1}\rangle_s$ and $\langle\cos\varphi_{n,n+1}\rangle_s$]. The results for the ac field decrement $\mathrm{Im}\{k_{ab}(B_y)\}$ are plotted in Fig. 8 as curves A, B, C, D, E, and G. At $\omega=0.7$ [for convenience, the frequency, temperature and energy are expressed here in units of the SC energy gap Δ_0 at $T=0$, while $\mathrm{Im}\{k_{ab}(B_y)\}$ is expressed in units of $(\Delta_0/c)\sqrt{\epsilon_\infty}$] the curves A [related to s wave symmetry of the order parameter, case (i)] and B [which itself corresponds to an anisotropic, d-wave order parameter $\Delta(\mathbf{p})$, case (ii)] behave in a similar way, while curve G [π stack, case (iii)] has an opposite tendency. From the last mentioned curves it follows that for the π stack, the decrement may turn to an increment, becoming negative, $\mathrm{Im}\{k_{ab}(B_y)\}<0$. One can also see, that at some values of field B_y, curve G crosses the zero axis, i.e., $\mathrm{Im}\{k_{ab}(B_y)\}=0$. It means that the ac penetration depth $\lambda_\perp^{\mathrm{ac}}(\omega,B_y)$ diverges at those points. Additionally from the curves A, B, and G one can note an attenuating oscillation of the decrement as field grows. This alternation is due to magnetic flux quantization in the system of stacked Josephson junctions. As the frequency increases up to $\omega=1.7$, the decrement diminishes for all the aforementioned cases (see curves C, D, and E). The calculations for a more realistic case of a larger single crystal with a size $L_x, L_y > \lambda_\perp, \lambda_J$ were performed at the same parameters as were listed before in comments to Figs. 6 and 7 (see Fig. 9). From Fig. 9 one can infer that the oscillatory behavior of the decrement may also take place for the larger sample as well. This kind of oscillation is related to deployment of regular fluxon chains into the sample. The curves are not as smooth as in the previous figure due to changes in topology of the vortex structure as B_y alternates. The above data suggest that $\mathrm{Im}\{k_{ab}(B_y)\}$ (and the penetration depth) of the ac electromagnetic wave is strongly affected by the applied dc magnetic field.

V. CONCLUSIONS

In conclusion, we have considered ac properties of layered SC's in a mixed state. We obtained that the dc magnetic field affects the Josephson and interference components of the ac current in presence of the pinned fluxon lattice. The found distribution of the supercurrent density corresponds to localized objects which can be identified as fluxons arranged in buckled chains being similar to the structure observed in the experiment.[18] As the field is increased, the structure changes its shape, and is washed out as fluxons overlap. The computed s-stack frequency-field dependencies of $\mathrm{Re}\{\epsilon^\perp(\omega,\mathbf{B})\}$ indicate that the resonance collective mode Ω_{ps} is suppressed by the applied dc field, but remains finite due to the ''extractive'' contribution. However, for the π stack, Ω_{ps} is reduced only at $B_y<0.06$, and then it begins to increase. We found that the finite dc magnetic field changes the ac current components leading to visible anomalies in the ac penetration depth $\lambda_\parallel^{\mathrm{ac}}(\omega,\mathbf{B})$, due to reactive properties of the fluxon lattice's environment. The results emphasize the importance of the intrinsic Josephson effect to determine the ac behavior of layered SC's in a dc magnetic field.

[1] K. Tamasaku, Y. Nakamura, and S. Uchida, Phys. Rev. Lett. **69**, 1455 (1992).

[2] C. C. Homes, T. Timusk, R. Liang, D. A. Bonn, and W. N. Hardy, Phys. Rev. Lett. **71**, 1645 (1993); D. N. Basov, T. Timusk, B. Dabrowski, and J. D. Jorgensen, Phys. Rev. B **50**, 3511 (1994); B. Koch, M. Durrler, H. P. Geserich, Th. Wolf, G. Roth, and G. Zachmann, in *Electronic Properties of High T_c Superconductors and Related Compounds*, edited by H. Kuzmany, M. Mehring, and J. Fink (Springer-Verlag, Berlin, 1990).

[3] A. M. Gerrits, A. Wittlin, V. H. M. Duyn, A. A. Menovsky, J. J. M. Franse, and P. J. M. van Bentum, Physica C **235-240**, 1117 (1994); Jae H. Kim, H. S. Somal, M. T. Czyzyk, D. van der Marel, A. Wittlin, A. M. Gerrits, V. H. M. Duijn, N. T. Hien, and A. A. Menovsky, *ibid.* **247**, 297 (1995).

[4] M. Tachiki, T. Koyama, and S. Takahashi, Phys. Rev. B **50**, 7065 (1994).

[5] L. N. Bulaevskii, M. P. Maley, and M. Tachiki, Phys. Rev. Lett. **74**, 801 (1995); L. N. Bulaevskii, V. L. Pokrovsky, and M. P. Maley, *ibid.* **76**, 1719 (1996); L. N. Bulaevskii, M. P. Maley, H. Safar, and D. Dominguez, Phys. Rev. B **53**, 6634 (1996).

[6] O. K. C. Tsui, N. P. Ong, Y. Matsuda, Y. F. Yan, and J. B. Peterson, Phys. Rev. Lett. **73**, 724 (1994); Y. Matsuda, M. B. Gaifullin, K. Kumagai, K. Kadowaki, and T. Mochiku, *ibid.* **75**, 4512 (1995); O. K. C. Tsui, N. P. Ong, and J. B. Peterson, *ibid.* **76**, 819 (1996); S. Sakamoto, A. Maeda, T. Hanaguri, Y. Kotaka, J. Shimoyama, K. Kishio, Y. Matsushita, M. Hasegawa, H. Takei, H. Ikeda, and Y. Yoshizaki, Phys. Rev. B **53**, R14749 (1996).

[7] L. J. Campbell, M. M. Doria, and V. G. Kogan, Phys. Rev. B **38**, 2439 (1988); S. N. Artemenko and A. N. Kruglov, Physica C **173**, 126 (1991); L. N. Bulaevskii, M. Ledvij, and V. Kogan, Phys. Rev. B **46**, 366 (1992).

[8] A. F. Volkov, Physica C **192**, 306 (1991); L. N. Bulaevskii and J. R. Clem, Phys. Rev. B **44**, 10 234 (1991).

[9] L. N. Bulaevskii, J. R. Clem, and L. I. Glasman, Phys. Rev. B **46**, 350 (1991); J. R. Clem, *ibid.* **43**, 7837 (1991).

[10] L. I. Glasman and A. E. Koshelev, Physica C **173**, 181 (1991); L. I. Glasman and A. E. Koshelev, Phys. Rev. B **43**, 2835 (1991); L. L. Daemen, L. N. Bulaevskii, M. P. Maley, and J. Y. Coulter, *ibid.* **47**, 11 291 (1993); Phys. Rev. Lett. **70**, 1167 (1993).

[11] A. Barone and G. Paterno, *Physics and Application of the Joseph-*

son Effect (Wiley, New York, 1982).
[12] S. E. Shafranjuk, M. Tachiki, and T. Yamashita, Phys. Rev. B **53**, 15 136 (1996).
[13] S. E. Shafranjuk, M. Tachiki, and T. Yamashita, Phys. Rev. B **55**, 8425 (1997).
[14] S. E. Shafranjuk and J. Keller, Solid State Commun. **78**, 1063 (1991); S. E. Shafranjuk and H. van Kempen, Phys. Rev. B **49**, 12 931 (1994).
[15] R. Kleiner, P. Müller, H. Kohlstedt, N. F. Pedersen, and S. Sakai, Phys. Rev. B **50**, 3942 (1994); S. Sakai, A. V. Ustinov, H. Kohlstedt, A. Petraglia, and N. F. Pedersen, *ibid.* **50**, 12 905 (1994); S. Sakai, P. Bodin, and N. F. Pedersen, J. Appl. Phys. **73**, 2411 (1993).
[16] A. L. Fetter and M. J. Stephen, Phys. Rev. **168**, 475 (1968).
[17] J. R. Clem and M. W. Coffey, Phys. Rev. B **42**, 6209 (1990); J. R. Clem, M. W. Coffey, and Z. Hao, *ibid.* **44**, 2732 (1991).
[18] G. J. Dolan, F. Holtzberg, C. Feild, and T. R. Dinger, Phys. Rev. Lett. **62**, 2184 (1989).
[19] B. I. Ivlev and L. J. Campbell, Phys. Rev. B **47**, 14 514 (1993).
[20] G. Rickayzen, *Theory of Superconductivity* (Willey, New York, 1965).